

**Supporting Information for**  
**Constructing Dynamic Na<sup>+</sup> Transport Channels in RT Na-S Battery Separators**  
**to Suppress Polysulfides Shuttling and Accelerate Reaction Kinetics**

*Xiaoxue Mao<sup>1,2</sup>, Zhiyong Xiong<sup>1,2</sup>, Yuhao Xiang<sup>1,2</sup>, Shihang Guo<sup>1,2</sup>, Xin Chen<sup>1,2</sup>,  
Hongyang Zeng<sup>1,2</sup>, Jian Jiang<sup>2</sup>, Sirui Wan<sup>1,2</sup>, and Yi Li<sup>3\*</sup>, Maowen Xu<sup>1,2\*</sup>*

<sup>1</sup>Chongqing Key Laboratory of Battery Materials and Technologies

<sup>2</sup>School of Materials and Energy, Southwest University, Chongqing 400715, China

<sup>3</sup>School of Chemistry, University of Nottingham, Nottingham NG7 2TU, U.K.

Email: [yi.li2@nottingham.ac.uk](mailto:yi.li2@nottingham.ac.uk); [xumaowen@swu.edu.cn](mailto:xumaowen@swu.edu.cn)

## **Experimental instruments and methods**

### **1. Characterizations**

The morphologies and structures of the MIL-121 and MIL-121/Na were observed by FESEM (JEOL JSM-7800F) and X-ray diffractometer (Bruker). The powder of MIL-121 and MIL-121/Na was determined by a Thermogravimetric analyzer (TGA, Q50, USA). Raman characterization was performed using a LabRAM HR Evolution (Horiba) Raman microscope with an excitation laser of 532 nm. The analyses for the specific surface area and the pore-size distribution were performed on Micromeritics under N<sub>2</sub> atmosphere by JW-BK-400.

### **2. Electrochemical measurements**

Tafel curve (Tafel), Cyclic voltammetry (CV), Linear sweep voltammetry (LSV), Electrochemical impedance spectroscopy (EIS) and i-t curve were measured on a CHI 760E electrochemical workstation. A battery test system obtained galvanostatic charge-discharge (GCD) curves (LAND CT2001A, China).

### **3. Ionic conductivity**

Ionic conductivity was measured by electrochemical AC impedance spectroscopy (EIS) in the frequency range from 1 kHz to 0.1 Hz with an AC amplitude of 100 mV via a CHI760E electrochemical workstation. The following equation calculated the ionic conductivity:

$$\sigma = \frac{L}{(R * A)}$$

L is the measured thickness, S is the facing area of the two stainless steel foils, and R is the horizontal intercept obtained from electrochemical impedance spectroscopy.

#### 4. Na ion transference number

Na ion transference number was measured utilizing an amperometric technique with an applied DC voltage of 20 mV and EIS measurement in a Na symmetric cell based on MIL-121/Na, MIL-121 and GF. The amperometric technique tested EIS before and after the DC polarisation. The  $t_{Na^+}$  value was calculated according to Bruce's equation:

$$t_{Na^+} = \frac{I_S(\Delta V - I_0 R_0)}{I_0(\Delta V - I_S R_S)}$$

where  $\Delta V$  is the polarization voltage (10 mV),  $I_0$  is the initial current, which is the steady state current,  $R_0$  is the initial resistance, and  $R_s$  is the steady state total resistance.

#### 5. Activation energy

The activation energy was calculated based on the Arrhenius relation with a linear fitting coefficient of over 0.99 after collecting electrochemical impedance at different temperatures. The Arrhenius relation:

$$\frac{1}{R_a} = A \exp\left(-\frac{E_a}{RT}\right)$$

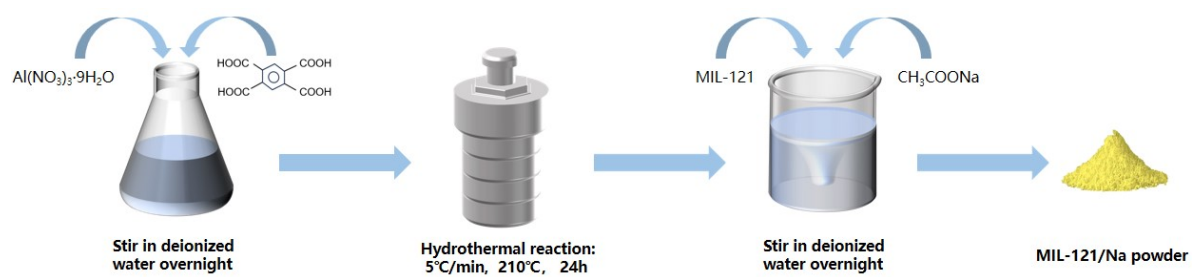


**Figure S1.** Schematic diagram of MIL-121 and MIL-121/Na synthesis process.

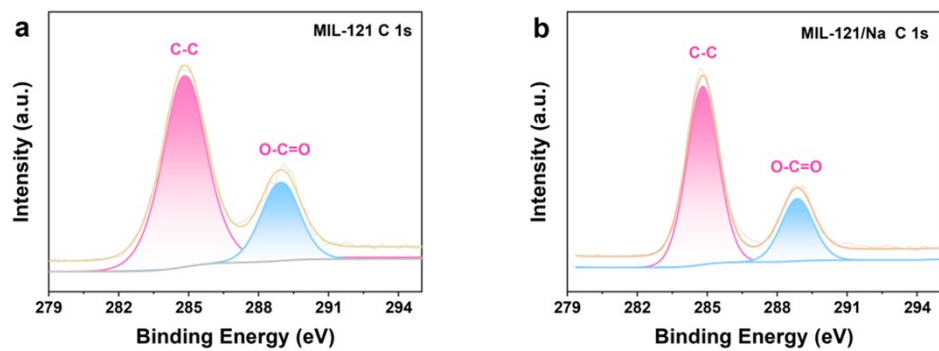


**Figure S2.** XPS spectra of C 1s of MIL-121 and MIL-121/Na.

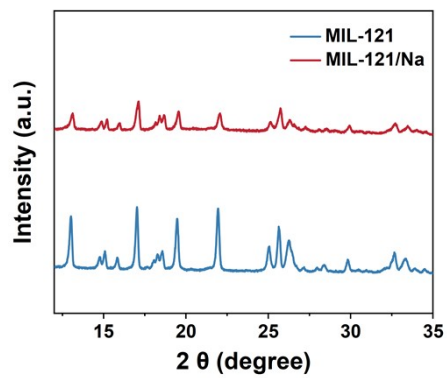


**Figure S3.** XRD of MIL-121 and MIL-121/Na.

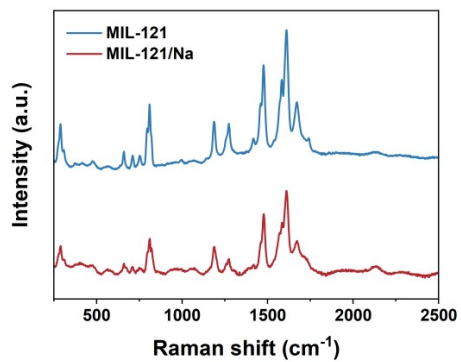


**Figure S4.** Raman of MIL-121 and MIL-121/Na.

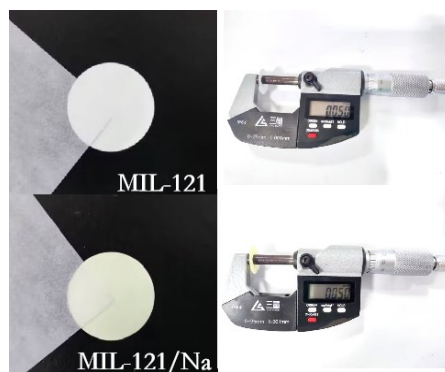


**Figure S5.** Thickness and color of MIL-121 and MIL-121/Na.



**Figure S6.** Image of MIL-121/Na separator flexibility.

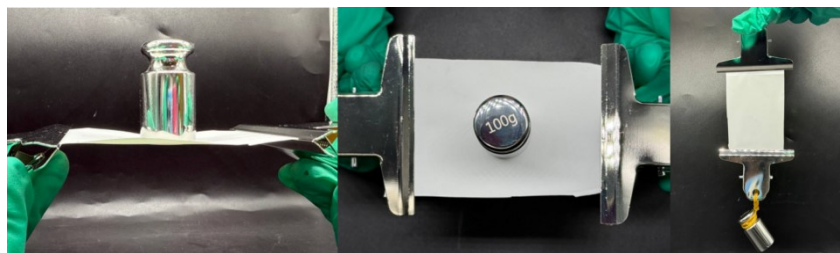


**Figure S7.** Tensile test of MIL-121.



**Figure S8.** Tensile test of MIL-121/Na.

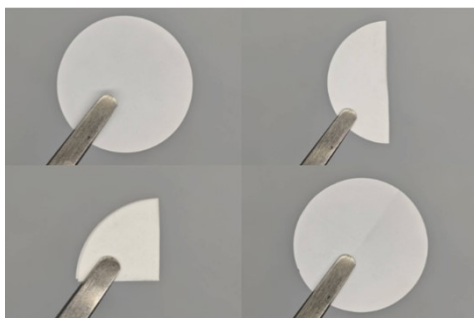


**Figure S9.** Digital images of the MIL-121 separator, single, double folded, and recovered.



**Figure S10.** Digital images of the GF separator, single, double folded, and recovered.

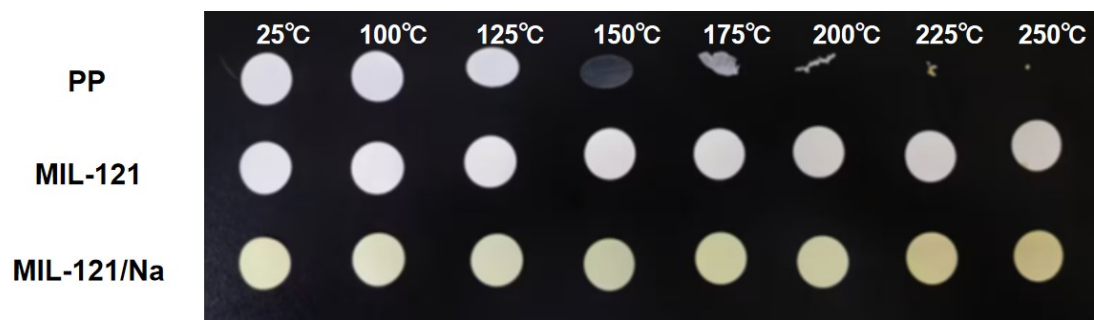


**Figure S11.** The heat shrinkage performance of PP, MIL-121, and MIL-121/Na.

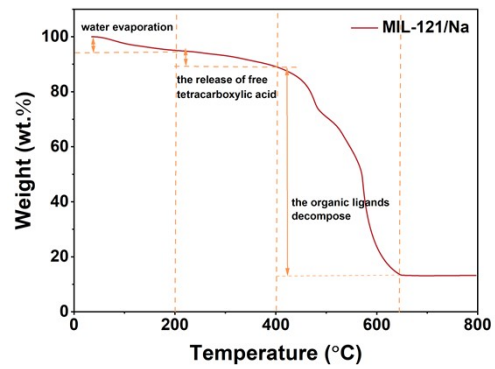
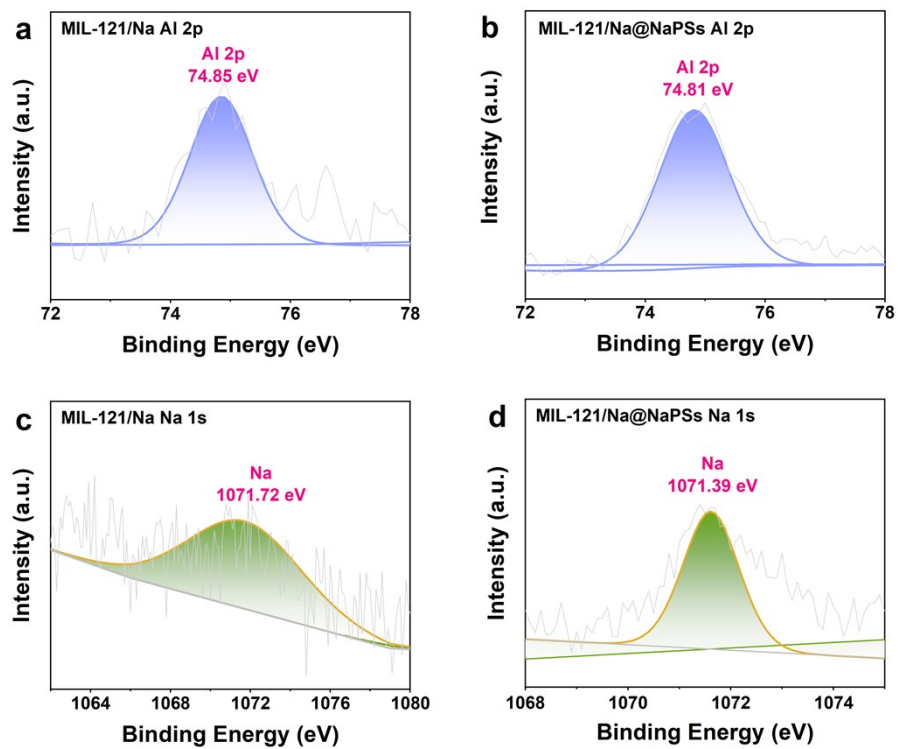
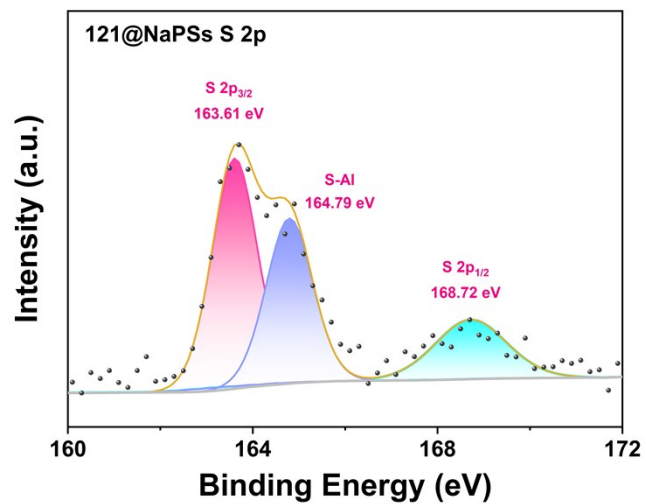


Figure S12. TGA of MIL-121/Na.



**Figure S13.** XPS spectra of a) Al 2p of MIL-121/Na, b) Al 2p of MIL-121/Na@NaPSs, c) Na 1s of MIL-121/Na and d) Na 1s of MIL-121/Na@NaPSs.



**Figure S14.** XPS spectra of S 2p of MIL-121 separator after the shuttle experiment test.

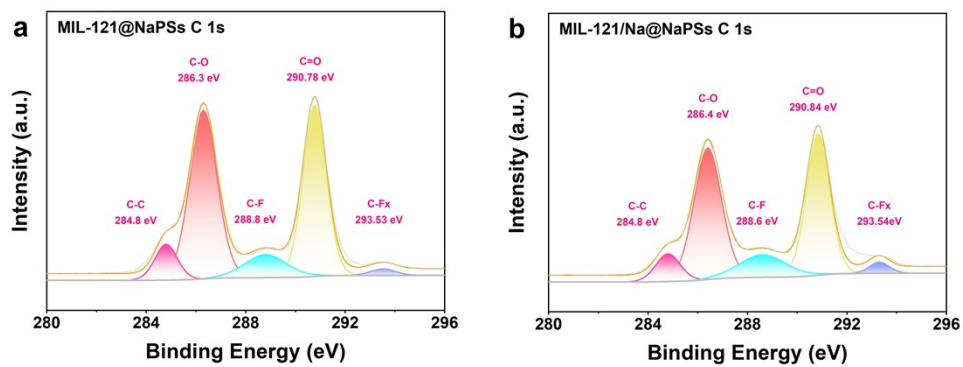


**Figure S15.** XPS spectra of C 1s of a) MIL-121@NaPSs and b) MIL-121/Na@NaPSs.

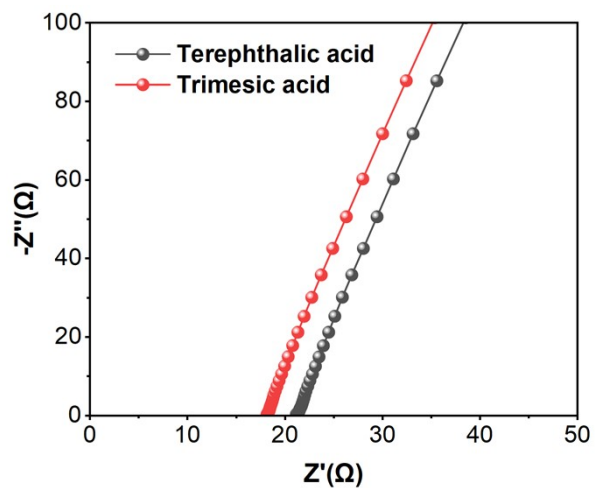


**Figure S16.** Ion conductivity of separators prepared with terephthalic acid and trimesic acid as constituents.

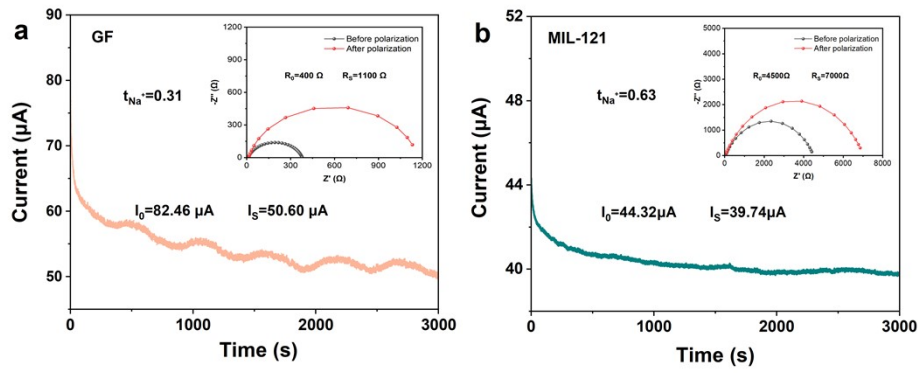


**Figure S17.** Electrochemical impedance spectra and direct-current polarisation curves of symmetric cells based on a) GF and b) MIL-121 separator.

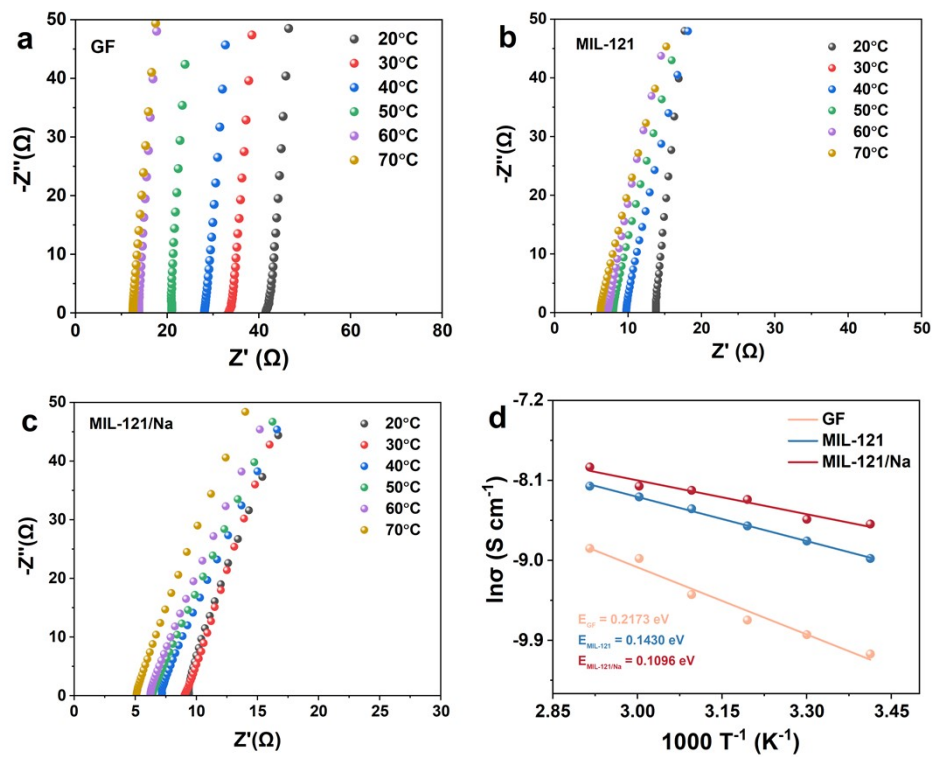


**Figure S18.** Electrochemical impedance spectra of a) GF b) MIL-121 and c) MIL-121/Na obtained at different temperatures. d) Arrhenius curves used to deduce the activation energy values for three membranes.

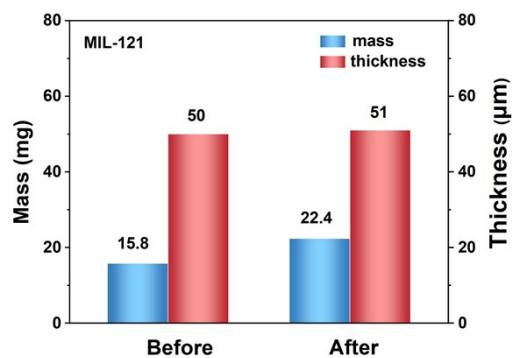


**Figure S19.** Variation of MIL-121 separator in mass and thickness after immersion in electrolyte.

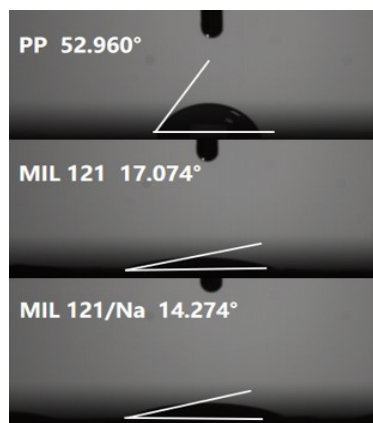


**Figure S20.** Contact angle test of PP, MIL-121, and MIL-121/Na separator.

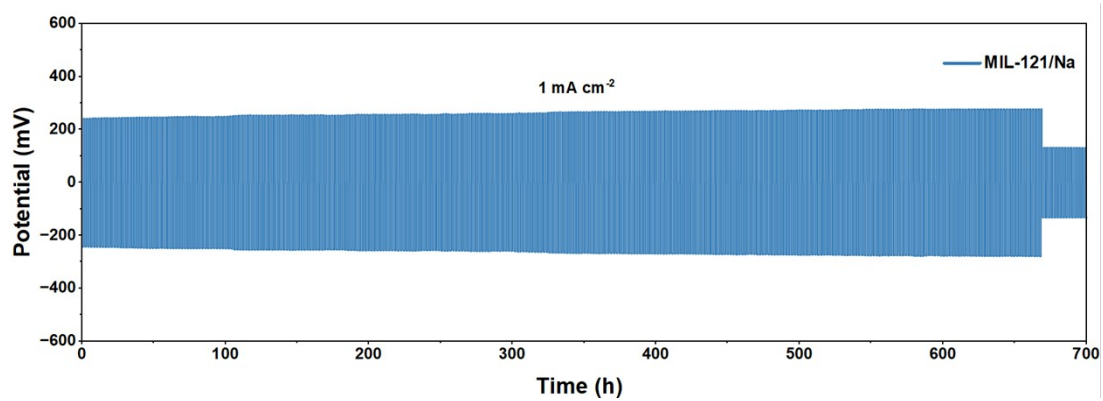


**Figure S21.** The long cycle of symmetrical cell with MIL-121/Na separator at  $1 \text{ mA cm}^{-2}$  current density.

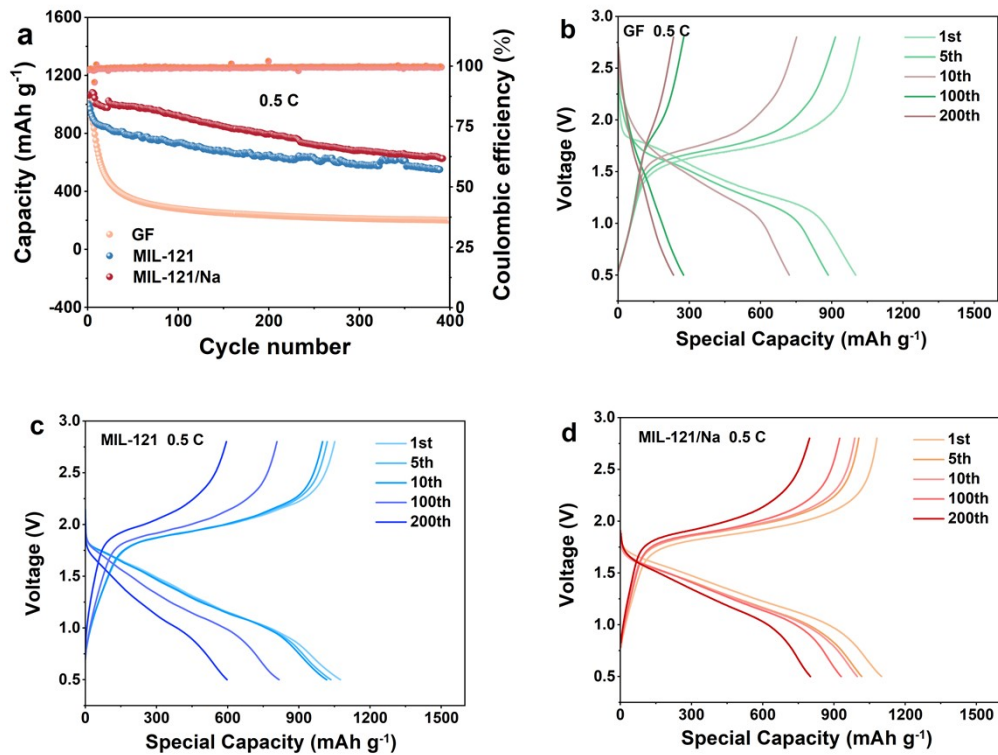


**Figure S22.** a) GF, MIL-121, and MIL-121/Na long cycle curves at 0.5C, b-d) and the specific capacity-voltage curves of the three at the 1st, 5th, 10th, 100th, and 200th cycles.



**Figure S23.** A pouch cell with a MIL-121/Na separator.

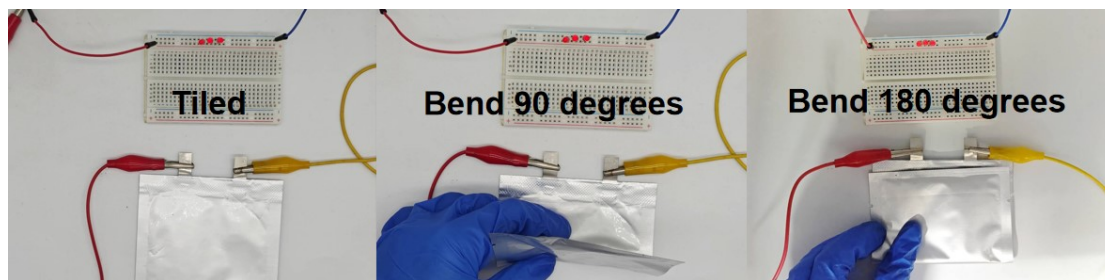


**Figure S24.** The pouch cell lights up the small bulb under tiling, bending 90 degrees and bending 180 degrees respectively.

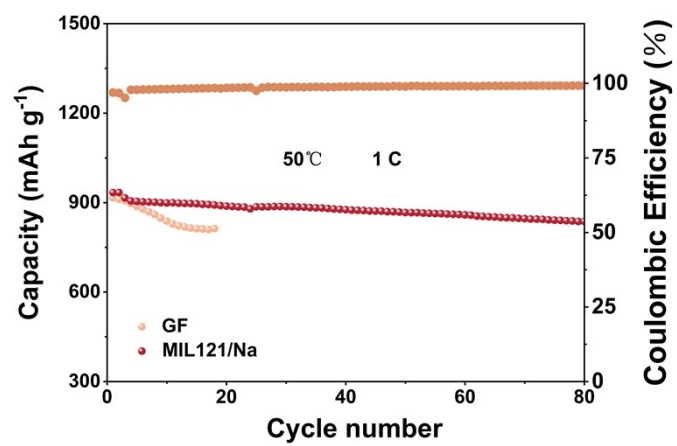


**Figure S25.** Long cycle curves of sodium-sulfur batteries with GF and MIL-121/Na separators at 1 C rate and 50 °C.